DIRECTIVITY AND PSYCHOACOUSTICS FOCUSED MULTI-OBJECTIVE DETECTABILITY OPTIMISATION FOR LOW NOISE ROTORCRAFT TRAJECTORIES

Bianca Erwee

Leonardo Helicopters, Lysander Road Yeovil
biancaemmaerwee@gmail.com

Nicolai Stadlmair, Daniel Redmann

Kopter Germany GmbH, Altlaufstr. 34, 85635 Hohenkirchen-Siegertsbrunn, Germany

ABSTRACT

This paper considers an advanced optimisation procedure for helicopter detectability as part of a typical approach trajectory. The objectives of the optimisation problem are formulated on the basis of two parameters: noise detectability threshold, and noticeability. Two key studies are undertaken, one purely looking at the optimisation of noise detectability – whether the noise is audible or not, and the other optimising between objective audibility and psychoacoustic noise perception. The detectability of the rotorcraft is then analysed for both cases and measured using a variety of microphone array configurations to investigate helicopter detection range and noise directivity control. These microphone points are the focus points of the optimisation procedure; the optimisation procedure utilises the strong changeability of helicopter noise directivity with trim condition to alter the flight path of the aircraft according to the placement of the microphones. Results within this paper have shown positive evidence that it is possible to optimise helicopter trim condition in flight to reduce helicopter detection and control noise directivity. Results also showed that for initial analyses, SEL and EPNL can be accurate and powerful tools for optimisation procedures to gauge annoyance in the absence of more sophisticated SQ metrics. The weightings given to the objectives within the objective function, and the calculation procedure for the costs associated with each objective were shown to strongly affect the optimal on-ground noise footprints. The relationships between the quantitative metrics used to encapsulate detectability were also found to strongly affect the results – and further study of the relationship between optimised values needs to be investigated in future work.

NOMENCLATURE

Abbreviations

BVI	Blade Vortex Interaction
MR	Main Rotor
TR	Tail Rotor
OASPL	Overall Sound Pressure Level [dB]
SEL	Sound Exposure Level [dBA]
SPL	Sound Pressure Level
SQ	Sound Quality
EPNL	Effective Perceived Noise Level
FW-H	Ffowcs Williams-Hawkings
SAMA	Surrogate Assisted Memetic Algorithm
ANN	Artificial Neural Network
GA	Genetic Algorithm

Tools

EMAA	Aerodynamics Solver
FAST	FW-H Far Field Acoustics Solver
HELENA	On-ground Noise Propagation Tool

1 INTRODUCTION

The conventional helicopter configuration (or 'Penny Farthing' design) is known for its highly characteristic noise signature – categorised most notably for its particular combination of impulsivity, loudness and tonality [1]. The uniqueness of the helicopter noise signature makes it typically simple to identify, and easy to detect at long range distances [2]. Psycho-acoustically, it also leads to helicopters being known as a great source of annoyance [3] – despite the overall noise levels often being little different to fixed wing aircraft [1]. Tactically, this leaves helicopters at a disadvantage, and more broadly suggests that the prediction of noise pollution on residents local to heliports is of particular importance [4].

In recent years research in helicopter acoustics has become increasingly popular as increased computational power has given rise to new and powerful numerical modelling approaches, and noise pollution has become a focus of concern. These technological improvements have led to the development of state of the art predictive acoustic methods, for certification activities. These new methods give a powerful opportunity to revisit helicopter detectability – at a time when helicopter noise sources & characteristics and human noise perception are both far better understood.

Previous work on Helicopter Detectability has been conducted predominantly by NASA and the U.S Air Force, in the 1970s and 1980s. This included work by Ungar et al [5], built upon previous work by Fidell et al [6], who proposed a method for quantitatively determining both fixed and rotary wing aircraft detectability distances. They proposed the development of a representative human aural detectability frequency curve, whose direct comparison with on ground frequency spectrums could determine whether a signal was detectable. Typically, the traditional auditory perception models used for aircraft detection analysis use computed representations of auditory critical band filters. These models attempt to locate a positive signal to noise ratio (SNR) in any singular band / group of bands and then apply classic signal detection theory to derive detectability measures (d prime, d') and probability of detection (POD) values for the event [7]. However, research into helicopter detectability in the 1970s [8] and research in the wind turbine sector on detectability and annoyance more recently has suggested that there is also a direct link between recognition of rotor noise and higher levels of annoyance. Helicopters have suffered from persistent noise complaints for decades now [9] [10]. The complaints have occurred despite the certification metrics for helicopters being defined by the same metrics as other fixed wing aircraft (in effective percieved noise level (EPNL dB) and Sound Exposure Level (SEL dB). The resulting conclusion must be drawn, that there are specific characteristics of the helicopter noise signature which increase the human annoyance response. Very recent work by a group of NASA researchers – who have been undertaking a range of research activities associated to rotorcraft annoyance over the last decade – has found through extensive auralisation modelling of helicopter noise & experimental testing that SEL and EPNL dB low noise optimised blade designs do not fully account for the annoyance percieved by the public [11].

In order to fully incapsulate the detectability problem therefore, this paper proposes a dual objective optimisation, focusing on both detectability and annoyance. In the following sections, the metrics defining these two objectives are formulated by consideration of the human auditory system, and implimented within the pre-existing approach trajectory optimisation tool developed by Cruz et al [3].

2 OPTIMISATION PROCEDURE

The optimisation procedure uses the method developed by Cruz et al [3], modified to work with a new advanced acoustic toolchain, as shown graphically below in the blue flow chart of Figure 1.

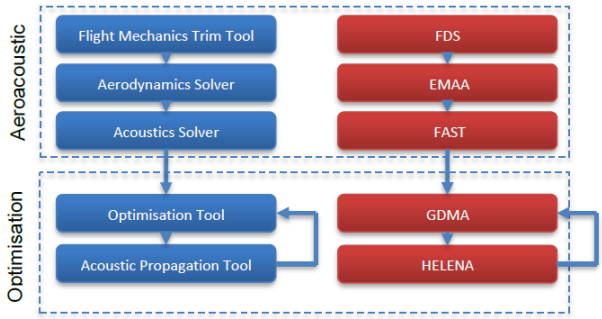

Figure 1 Modified aeroacoustic optimisation computational process

The method can be considered in two parts: the assembly of the acoustic database, and flight path optimisation procedure. These can be described as follows.

2.1 Acoustic Database Assembly

The acoustic database, generated using the aeroacoustic toolchain shown in Figure 1, is pre-calculated using hemispheres below the rotorcraft to capture their noise signature and directivity. The database consists of a predetermined set of helicopter trim conditions, sufficient in resolution to describe all possible optimised trajectories within the path constraints placed on the model.

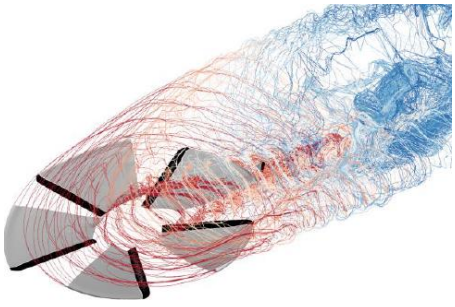

Figure 2 Aerodynamic Solver EMAA Graphical Output

The method was adapted to work with Leonardo's rotorcraft aerodynamics and acoustic simulation toolchain (EMAA, FAST). The new method is capable of modelling the interactional effects between multiple rotors, allowing the simulation of the coupled main rotor tail rotor case. An example of the graphical output from the aerodynamic solver is shown above in Figure 2.

For the database created in this work, a sweep of speeds from 50-100kts and degrees of descent 0-12 degrees were used based on previous analysis procedures by Cruz et al [3] for the optimisation of the approach condition.

2.2 Flight Path Optimisation Algorithm

The optimisation algorithm is a Surrogate Assisted Memetic Algorithm (SAMA), chosen for the coupled global and local search approach it applies – which enables the entire design space to be explored, whilst allowing for computationally efficient small local improvements. The algorithm employs a Genetic Algorithm (GA) as the global search algorithm, and a gradient based algorithm for local improvements, designed to optimise the objective function using a surrogate model of the function itself. This Surrogate Model is generated by an Artificial Neural Network (ANN).

The optimisation procedure uses the acoustic database to analyse different paths by passing the on-ground propagation tool (HELENA) the desired path trajectory and associated hemispheres. A set of 'flyability' metrics were set considering the flight mechanics of the aircraft, to ensure optimal paths are practically achievable. By limiting the acceleration, rate of descent and vertical speed gradient of the path (adding a cost to the objective function for paths exceeding these limits), the code ensures that the optimised flight path is flyable by the modelled aircraft.

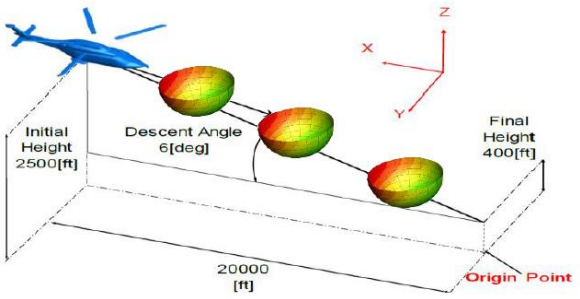

Figure 3 Trajectory Optimisation Strategy Using Acoustic Hemispheres

The original version of this optimisation method was designed for the optimisation of the on ground noise footprint of a helicopter in the 80kt, 6 degree approach condition – which is known to be BVI laden for conventional configurations. The aim was to minimise noise directly below the aircraft – using certification noise metrics (SEL and OASPL dBA) to define the optimisation objectives in noise reduction. To reduce the unknown factors related to the redefinition of the optimisation procedure for detectability, the following optimisation analysis uses the same baseline approach trajectory as the original tool developed by Cruz et al [3]. The approach trajectory also provides an opportunity to analyse the psychoacoustic impact of noise impulsivity – prominent in the approach condition where Blade Vortex Interactions (BVI) are common and predicted by the tool. This method is shown graphically in Figure 3.

In order to optimise for helicopter detectability, a number of changes to the optimisation approach must be considered. Most prominently, this can be split into two parts, which concern the definition of the optimisation objectives:

1. Direct Objectives: *Defining the objective function*
2. Indirect Objectives: *Altering the microphone array to change the focus of the optimisation.*

The process by which these objectives are applied within the optimisation is shown graphically in Figure 4. The indirect objectives, such as the microphone array configuration, are not actively optimised but the optimisation procedure is highly sensitive to their definition. As such their setting also has the power to significantly alter the result of the optimisation.

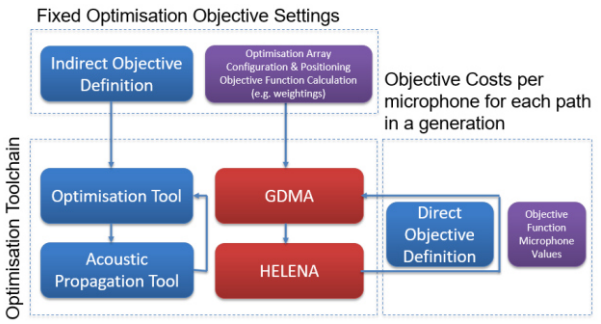

Figure 4 Configuration of the Detectability Optimisation Objectives

Conversely, the direct objectives, which form the objective function, can be a number of metrics which are compromised between within the optimisation loop. The optimisation therefore actively aims to improve these characteristics (in this case detectability and annoyance metrics). How these objectives have been defined is described further in sections 3 & 4.

3 OBJECTIVE FUNCTION DEFINITION

The certification approach optimisation proposed by Cruz et al [3] is capable of handling Multi-Objective Optimisation Problems and works using 2 objectives:

1. Minimisation of the maximum SEL value on ground (dBA weight correction)

2. Minimization of the on-ground noise footprint in terms of SEL metric (dBA weight correction). This objective is improved by reducing the ground area in which the SEL value is higher than a threshold value

These objectives manipulate the SEL microphone measurements to tune the optimisation solutions.To optimise for detectability these objectives have to be redefined, and metrics quantifying signal detection outlined. This is described as follows.

3.1 Quantifying Detectability and Annoyance

There are predominantly two factors which must be considered when modelling human noise detectability:

- Noise detectability threshold
- Noticeability

The first can be calculated based on the frequency sensitivity of the human auditory system. This sensitivity is closely related to critical bands which can be used to quantify the ability of the human ear to distinguish between individual frequency tones. This phenomena is created by the cochlea – the hearing organ within the ear – which has a logarithmic spiral shape that governs the ability to distinguish between frequencies [12]. In the presence of background noise, classical signal detection theory based on signal to noise ratio analysis can be applied to determine the masking effect of the additional noise.

The second relates to the subjectivity of human noise perception. Studies have shown that there is a clear correlation between annoyance and the noticeability of a given sound [13], [14]. The more annoying the sound, the more likely the observer is to notice it – most critically at lower levels of sound close to the detection threshold, where the sound could be more easily dismissed [15].

As such, methods to quantify both classic signal detectability and human 'perceptibility' of that signal have been considered, and defined as follows.

3.1.1 Detectability Threshold

The noise detectability threshold can be simply defined as the noise value above which a given noise signal can be considered audible to the human ear.The following analysis uses a method decribed by Ollerhead et al [16], which was subsequently used in the development of a helicopter detectability prediction tool developed by NASA at least up until 2008, called AUDIB, and based originally off work as part of the I Can Hear It Now (ICHIN) program to calculate the human noise detectability threshold. The method is as follows:

1. Convert helicopter noise signal and ambient noise signal from 1/3 octave band levels (L_n) to critical band width levels (M_n). The comparison between the two filters shows the close correlation between the two metrics – the only difference between the two is in precise bandwidth – which is slightly wider for the frequency bins below 250Hz.

   As such, the conversion to effective critical band width levels uses Equation 8 for frequencies below 250Hz ($n < 14$), for which critical band widths are wider than the 1/3 octave bands. The SPL values at these frequencies must be calculated as a sum of the total or partial energies from a number of adjacent 1/3 octave bands.

   (1) $L'_n = \sum_{i=1}^{14}[L_i + B_i\,]$
   where $L_i = L_n$ for $i = n$

   Above 250Hz, a simple increment is applied to the 1/3 octave level: $L'_n = L_n + R_n$.
   Incremental values B_i and R_n are taken from tabulated results from Ollerhead [16].

2. Calculate the combined critical band threshold level (T'_n) at each frequency as the decibel sum of the absolute threshold (A'_n) and the masking threshold (M'_n).

   (2) $T'_n = A'_n + (M'_n - 5)_{dB}$

   If the difference between A'_n and $M'_n - 5$ exceeds 13dB, it is sufficiently accurate to put T'_n equal to the greater of A'_n and $M'_n - 5$. Values for A'_n at each 1/3 octave band are given as tabulated values by Ollerhead et al [16].

3. Subtract the combined threshold value from the critical band signal levels. If the value is above 1dB, it can be considered audible.

However, this paper intends to concentrate on an initial investigation of the objective function, focusing on the sensitivity of the optimisation procedure with this new metric, and the tradeoffs between detectability and annoyance. This paper has therefore omitted an investigation into the masking effect – modelled here in Step 2 of Ollerheads proposed method, which essentially means that $M_n' = 0$.

This allows for an independent analysis into the noise characteristics of the helicopter profile, before considering how the signal to noise ratio of a given environment may effect the detectability of an aircraft. Further research may look at this effect – using signal to noise algorithms to add pink noise to the noise spectrum. This will also effect the calculation of Fluctuation Strength, which is directly dependant on the masking depth of the signal.

3.1.2 EPNL & SQ Metrics

The A-weighting typically applied to SEL dB calculation for certification of light helicopters in the flyover condition is known to have limitations in its prediction of subjective noise evaluation, as its frequency dependence corresponds only to that of the equal-loudness contours at low levels up to 65dB.Therefore, dBA values of noises or complex tones, or combinations of both, can be misleading when used as indications of subjectively perceived loudness [17].

EPNL is perhaps one of the most well-known metrics for measuring human noise perception in aviation – the acronym itself being 'effective perceived noise level' - and a measure used for the louder certification conditions of heavier aircraft.

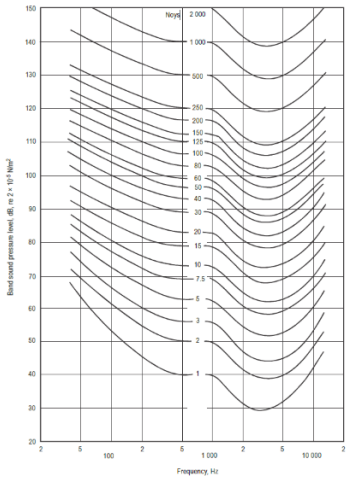

Figure 5 EPNL Noise Correction Graph showing Equal Loudness Contours **[18]**

EPNL dB is calculated based on PNLT – where PNL is the corrected perceived noise level calculated using equal loudness contours shown in Figure 5, and PNLT adds the pure tone correction factor (C). The variance of (C) with frequency and level difference is shown below in Figure 6.

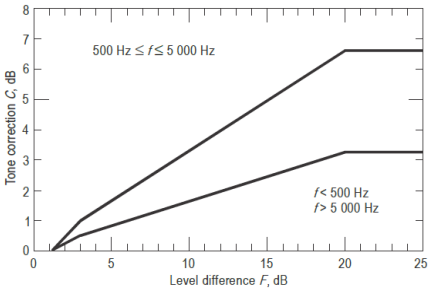

Figure 6 Tone Correction Factors **[18]**

It also takes into account noise duration – accounting for a 10 dB down period. As such, it has for many years been considered to be sufficient in capturing the impact of aircraft noise on the public psyche.

Recent work by NASA however, researching the cause of rotorcraft annoyance, has outlined that SQ metrics have the ability to better capture the noise perception of rotorcraft [11]. Of the SQ metrics considered: loudness, impulsivity, roughness, fluctuation strength, tonality and sharpness, tonality, sharpness and fluctuation strength showed the largest effects independant of the loudness of the noise source. As tonality and subjective loudness are already accounted for EPNLdB, sharpness and fluctuation strength must be considered as the SQ metrics of most interest. Fluctuation Strength, a measure of the aperiodic fluctuation of amplitude or frequency within a signal, has been more strongly linked with detectability, and hence is the preferred metric to use in this optimisation analysis.

However, fluctuation strength requires the original time series for each microphone in order to perform the necessary fourier transform and inverse fourier transform – which is not currently provided by HELENA.

In the absence of this output, it is considered beneficial to consider other variables which may serve as an indicator of fluctuation strength from an optimised result. Since the modulation frequency, on which fluctuation strength strongly depends, cannot be calculated it is impossible to know the correlation factor between fluctuation strength and SPL – preventing it's direct optimisation within the objective function. However, experimental results have shown strong indications of positive correlation between SPL and Fluctuation Strength.

An example of this correlation activity is shown below in Figure 7 produced from experimental research by Fastl and Zwicker [12].

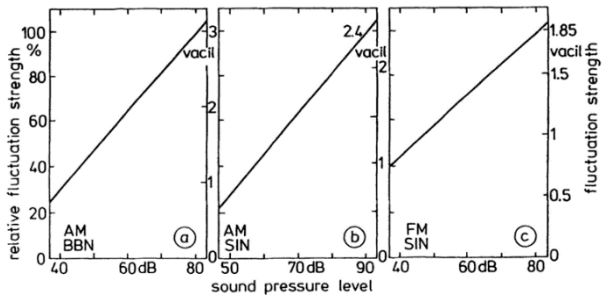

Figure 7 Fluctuation Strength as a function of SPL for (a) amplitude modulated broadband noises (b) amplitude modulated tones and (c) frequency modulated tones; modulation frequency of 4Hz **[12]**

As such, the focus of this study is to investigate improvements in SPL by measuring SEL as well as the objective function parameters, as an initial view into the optimisation output – and the effectiveness of the detectability threshold factors in reducing overall noise (as would be expected).

Since tonality and loudness are already accounted for within the EPNL dB metric, initial results are therefore run optimising EPNL dB as the annoyance metric - with a view to replacing / adding to this metric when time series data can be made available.

3.2 Objective Function Formulation

Using the calculation procedures defined above for the detectability threshold & EPNLdB, two optimisation objective formulations have been divised. For the first formulation, the objectives are:

1. Average detectability factor
2. Maximum detectability factor

The average value is taken based on the average amplitude of each 1/3 octave frequency band over the total flight time for which the microphone is recorded. The maximum value is then taken based on the maximum amplitude for each 1/3 octave frequency band, over the flight time of the helicopter. Certification metrics are typically only evaluated over the 10dB down period. However, for the case of detectability the loudness of individual frequency components must be considered, for the full duration of the helicopter flight. This is due to the nature of detectability, as we cannot safely negate areas where helicopter noise is perceivably lower than the maximum but still detectable – these areas will affect the overall detectability of the aircraft.

Both objectives are given equal weightings in the optimisation procedure. The optimisation code also includes a threshold parameter, which defines a baseline value for each metric below which the parameter is considered to be optimal. Changing this parameter can have a large effect on the sensitivity of the optimisation code – particularly if the threshold is set too high, resulting in a quasi-single objective function. The cost function for each parameter is as follows:

$$(3)\quad C = C + 1 \qquad if\ m_i > T_N\ \&\ m_{i-1} > T_N$$

$$(4)\quad C = C + 1 - \frac{T_N - m_{i-1}}{m_i - m_{i-1}} \qquad if\ m_i > T_N\ \&\ m_{i-1} < T_N$$

$$(5)\quad C = C + \frac{T_N - m_{i-1}}{m_i - m_{i-1}} \qquad if\ m_i < T_N\ \&\ m_{i-1} > T_N$$

Where C is the cost of the objective, T_N is the noise threshold,and m_i is the i^{th} microphone parameter.

The second formulation is:

Objective 1: *EPNLdB*
Objective 2: *Maximum Detectability Factor*

Which uses the same cost function & threshold formulation as the first formulation, described by equations 3,4 and 5.

4 INDIRECT OBJECTIVE DEFINITION

The area below the aircraft to be minimised can be altered by changing the microphone array used in the optimisation. The code is limited computationally to an array of approximately 61 microphones, thus limiting possible configurations. The aim is to investigate a number of different array configurations, and position this array at different points along the helicopter flight path.

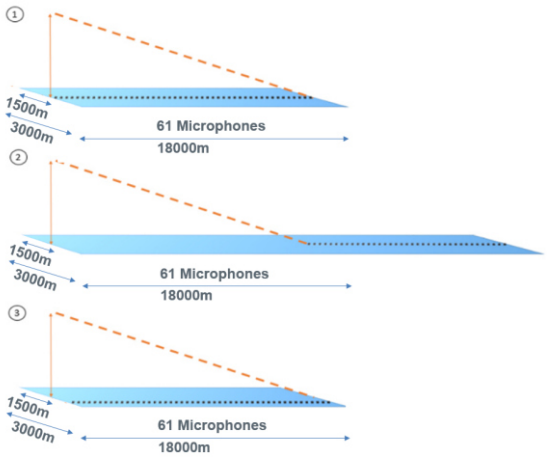

Figure 8 Microphone array optimisation placements at 1) the centreline, 2) the 18000m in front of the helicopter landing point, 3) 500m to the right of the centreline

The aim is then to examine the optimised change in flight path, used to control the directivity of the helicopter – and examine the difference in effective avoidance with the array positioning. An initial set of array configurations which will be investigated are shown above in Figure 8.

5 RESULTS

The following results section is split into 2 sections, based on the defined objective functions:

1. Detectability threshold maximum vs average
2. Max detectability threshold vs EPNL dB

Section 1 covers if and how helicopter noise detectability can be optimised – and the sensitivities of the optimisation procedure. Section 2 performs an initial evaluation of detectability & EPNL dB optimisation.

5.1 Detectability Study – Average vs Max

For the following analysis, consider all references to objectives 1 and 2 to refer to the average and maximum detectability factors respectively. The microphone array configurations will be referred to as numbered above in Section 4. An initial sensitivity study, undertaken to understand the optimal settings for the optimisation procedure – the results of which are not presented here – concluded that solutions provided converged results after 40 generations, with threshold parameters (15,65) for the average and maximum detectability parameters respectively. All results presented here therefore use these settings.

5.1.1 Microphone Arrangement 1

The objectives cost for every path solution developed by the optimisation tool is shown below in Figure 9. The pareto front for this problem is wide – and shows a linear trend between the maximum and average detectability factors – that for the optimal cases one will decrease for the other to increase.

Of the many points on the pareto front of this solution, 5 points spanning the full breadth of solutions and describing the trend in changing noise footprint with objective costs have been chosen. The ΔdBA SEL noise footprints for these solutions are shown in Figure 10. The footprint is only shown in these cases for the main rotor noise sources, which account for the major changes in noise with trim condition – and thus give an accurate initial trend study. These solutions will hence be referred to as Pareto 1 – 5, in the order they appear from top to bottom in Figure 10.

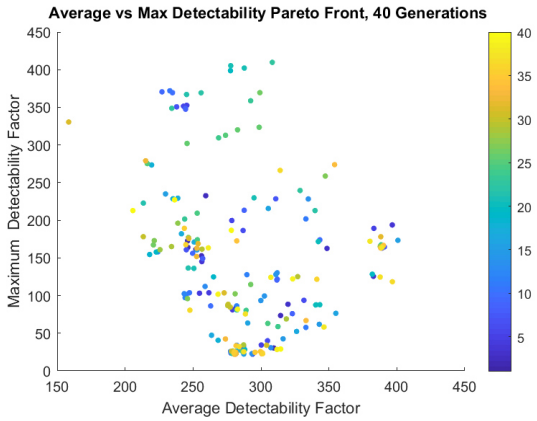

Figure 9 Pareto Front Objective Function Solutions for Average / Maximum Detectability Factor, with microphones beneath the Helicopter for 40 generations

These results show that the higher the cost of objective 1 – the average detectability factor – the more polarised the resulting footprint becomes. Pareto 1 shows a strong reduction in noise around the microphone centreline, but results in a slight increase to the right of the helicopter.

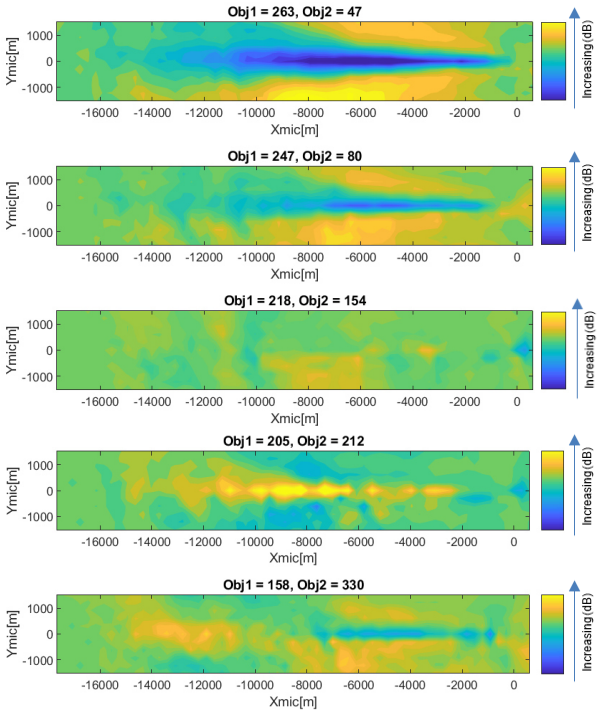

Figure 10 Pareto Solutions showing MR ΔdBA wrt baseline for the trajectory optimisation using maximum and average detectability factors after 40 generations

Comparatively, opting to minimise the maximum detectability factor – such as the solution given by Pareto 5 – results in noise reductions less directly related to the microphone positioning, and generally

more evenly distributing the noise over the footprint. The helicopter also shows a tendency, as it flies from left to right, to shed more noise to the right of the aircraft than to the left – this behaviour is to be expected, given that it corresponds with the advancing side of the helicopter rotor blade. The advancing blade is subject to increased noise emissions from BVI and high speed effects.

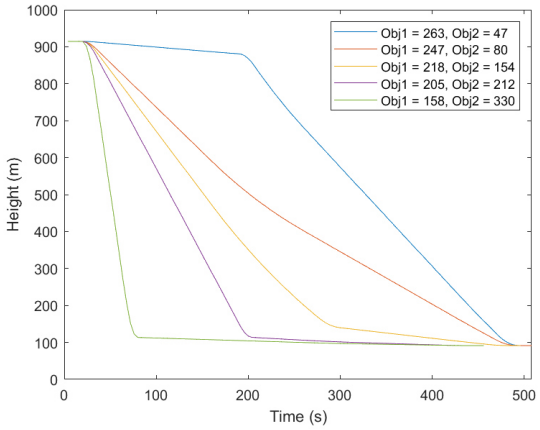

Figure 11 Altitude Profiles for the Pareto Solutions of the maximum / average detectability trajectory optimisation after 40 generations

In order to give more insight into the trajectory optimisation procedure itself, the path trajectories for all 5 pareto solutions given in Figure 11 are plotted in Figure 12 for time vs height and speed. These results show that the optimal trajectory required to maximise the detectability factor is gradual in both speed reduction and rate of descent. Conversely, to maximise the average detectability factor, (thus generating a more polarised noise footprint), the helicopter descent path is steeper and faster.

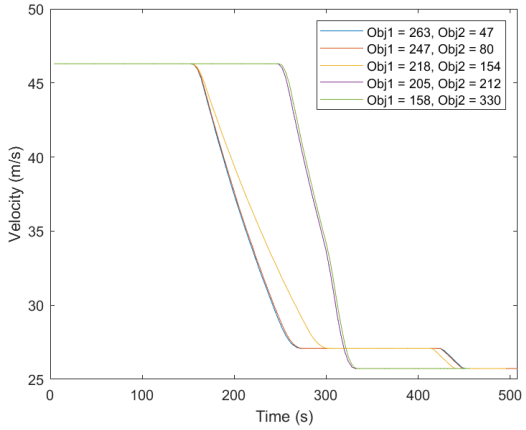

Figure 12 Velocity Profiles for the Pareto Solutions of the maximum / average detectability trajectory optimisation after 40 generations

The footprints of the objective functions were calculated for the optimal pareto solution, Pareto 2, as shown in Figure 13. The results show that the maximum detectability of the helicopter occurs between x = -6000m and x = -2500m. At these points, the helicopter goes from 628m to 284m, at 52kts. There is also a noticeable correlation between the A weighted loudness measure (SEL) and the average detectability threshold factor, suggesting that SEL may be used to minimise detectability.

Additionally, the solution shows a slight bias in increased detectability towards the left side of the helicopter, despite the ΔSEL values for the MR showing an increase in noise on the right of the rotor. This suggests that the noise levels are the same and that the difference is in spectral content between the two sides. This may be explained by BVI noise, which introduces increased impulsive noise between 300-1000Hz and would be more sensitive to the human auditory system.

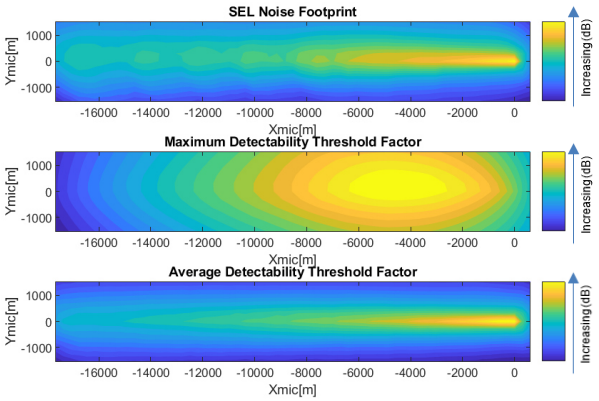

Figure 13 Footprint of Objective Functions calculated for a larger grid (rather than the central microphone line used within the optimisation loop) for pareto solution Obj1 = 247 Obj2 = 80 and compared to the total SEL noise footprint for the helicopter

5.1.2 Microphone Arrangement 2

The following analysis measures the effectiveness of the trajectory tool to minimise noise in front of the helicopter landing point. This optimisation has a very narrow pareto front, resulting in just one primary optimal solution. The change in SEL values (by comparison and delta) between the baseline and optimised approach condition is shown in Figure 14. This graph shows a reduction in noise up to 8km away, with a notable decrease within the first 500m.

The predicted range of the helicopter noise is noticeably high – and this may partly be a result of the limitations in HELENA's atmospheric modelling, which only accounts for ideal atmospheric absorption. It may therefore overestimate the noise propagation of the helicopter noise signature over such a long distance. However, in this case the SEL footprints only give an indication of annoyance /

fluctuation strength – in terms of actual detectability, the most telling graph is shown below in Figure 15.

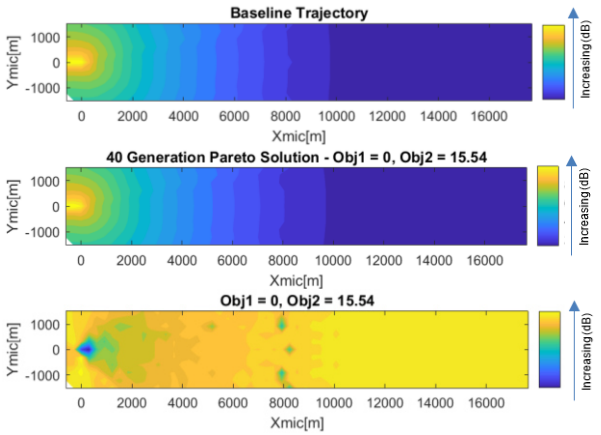

Figure 14 Reduction in MR SEL in front of the helicopter using Max / Average Detectability Objectives, with 40 generations

This graph shows the maximum detectability factor – and therefore shows the highest noise which is above the noise threshold for a given frequency. It therefore gives us a prediction for the detection range of the helicopter as it performs a given trajectory, and the outlines that the code has the potential to optimise this detection range.

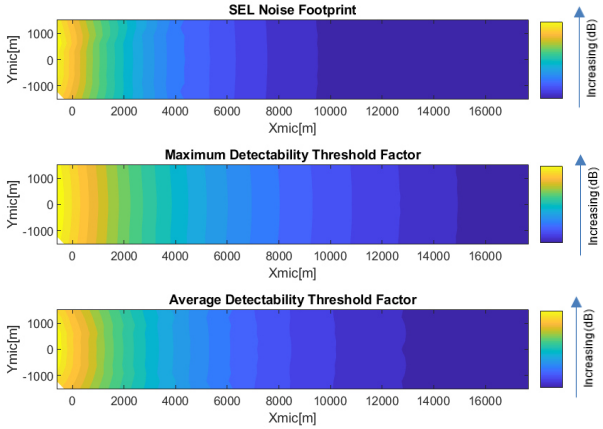

Figure 15 Footprint of Objective Functions calculated for a larger grid in front of the helicopter landing point (rather than the central microphone line used within the optimisation loop) for the Pareto solution and compared to the total SEL noise footprint for the helicopter

In order to appreciate the connection between the detectability threshold and the strength of each frequency within the helicopter signature – and how it decays with time – the MR spectrogram for this pareto solution is plotted in Figure 16. This spectrogram shows the microphone recording in 1/3 octave bands at 2133, 8230 and 14325m for microphones 10, 30 and 50 respectively.

The spectrogram shows the numerical decay in maximum noise SPL from 2 to 18km from the helicopter landing spot. As would be expected, the spectrogram shows that it is the lowest frequency between 50 – 63Hz which propagates furthest without losing energy. Analysing and comparing the 2km case – which is at the threshold of human hearing for most of the time – with the 8km case shows that it is the frequencies above 200Hz that drastically affect the detectability of the helicopter.

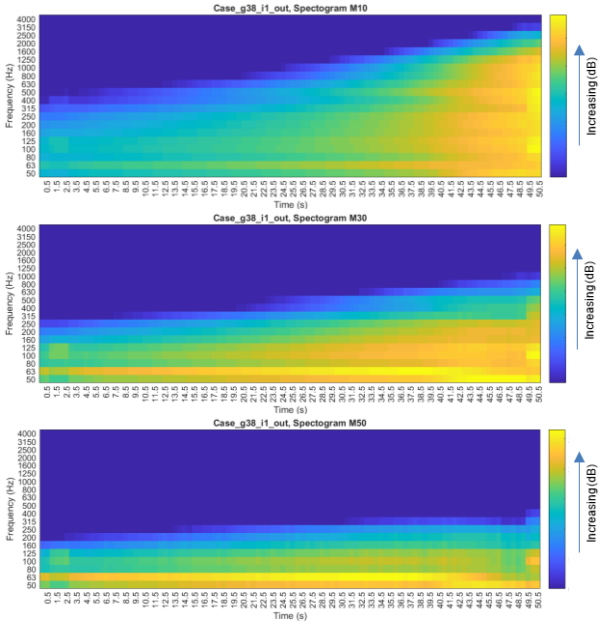

Figure 16 Spectrogram of Main Rotor Front Line Optimisation Microphones 10, 30 and 50

Consequently, it can clearly be seen from Figure 17 – showing the spectrogram of the TR – that the detectability range of the rotorcraft is dependent on the main rotor and not the tail rotor.

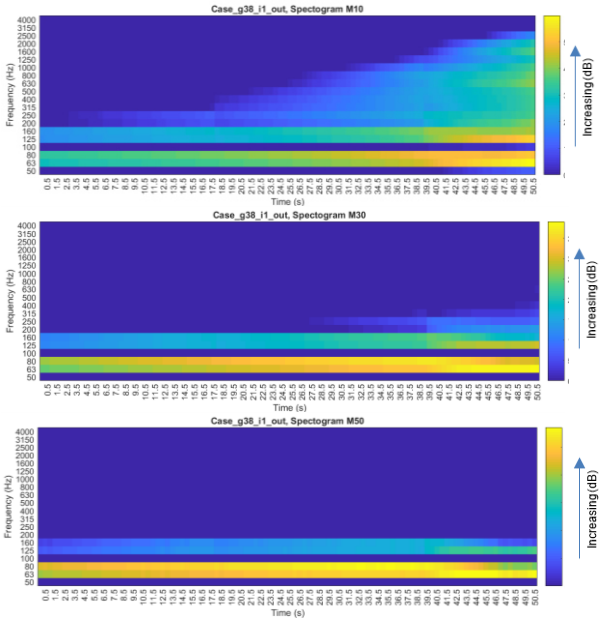

Figure 17 Spectrogram of Tail Rotor Front Line Optimisation Microphones

This is because the tail rotor does not generate the strong mid-to-low frequencies which propagate powerfully through the atmosphere and are generated by the main rotor.

5.1.3 Microphone Arrangement 3

The following analysis uses microphone arrangement 3 to analyse the ability of the optimisation tool to minimise noise to the right of the helicopter flight path. This optimisation has a very wide pareto front, which is rectangular in nature – this suggests that there exists an impasse between the two objectives in this case, whereby either one or the other may be optimised and improvements in both objectives is limited early on.

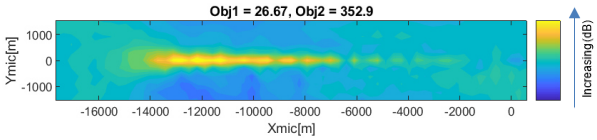

Figure 18 MR Delta between the SEL Pareto Solution 1 and the baseline approach

The optimal pareto solutions were analysed first using an SEL comparison with the baseline trajectory case. The results show only one pareto solution which successfully optimised the rotor trim condition to reduce noise to the side of the helicopter – pareto 1 (Obj1 = 26.67, Obj2 = 352.9). The delta SEL plot wrt to the baseline trajectory for this solution is shown below in Figure 18.

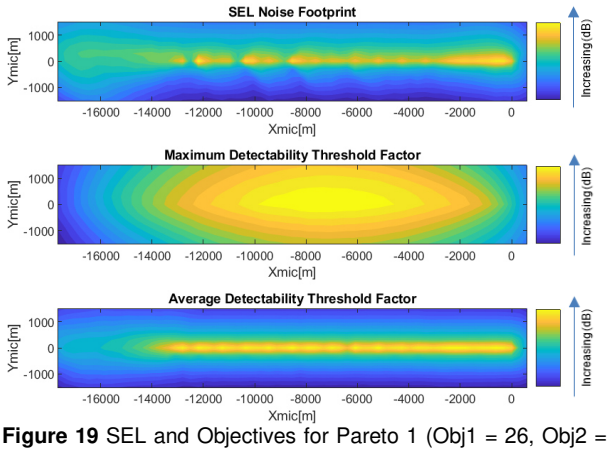

Figure 19 SEL and Objectives for Pareto 1 (Obj1 = 26, Obj2 = 352)

The pareto 1 optimal solution has also been analysed for the full MR/TR SEL footprint, maximum and average detectability factors as shown graphically in Figure 19. This result shows that the optimisation tool was able to successfully control the directivity of the helicopter rotor noise such that the noise on the right side of the helicopter flight path is reduced.

5.2 Detectability & EPNL dB

The following analysis uses microphone arrangement 1 to perform an trajectory optimisation optimising EPNL dB and the maximum detectability threshold factor. Figure 20 below shows the pareto front for this optimisation procedure, which is very narrow in this case – resulting in one optimal solution. This is partly due to the definition of the threhold values – which were set at 70 and 65 for the EPNL and threshold detectability parameters respectively. The same number of generations (40) were used for this analysis.

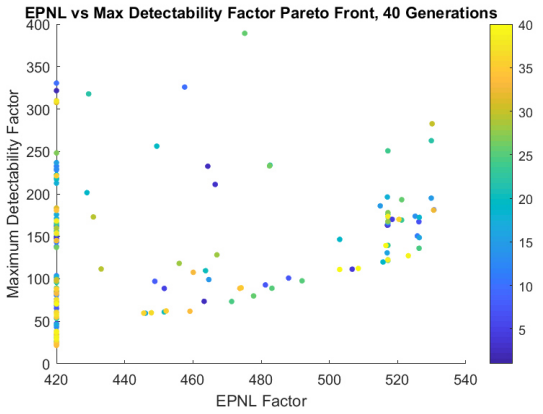

Figure 20 Pareto Front Objective Function Solutions for EPNL / Maximum Detectability Factor Objective Costs, 40 Generations and Microphones below the helicopter approach path

The optimisation of the EPNL footprint for the optimal pareto front solution is shown below in Figure 21. The result shows a larger difference between maximum and minimum noise values, with the noise at the optimisation microphone positions lowered at the expense of the increase in noise over the surrounding area.

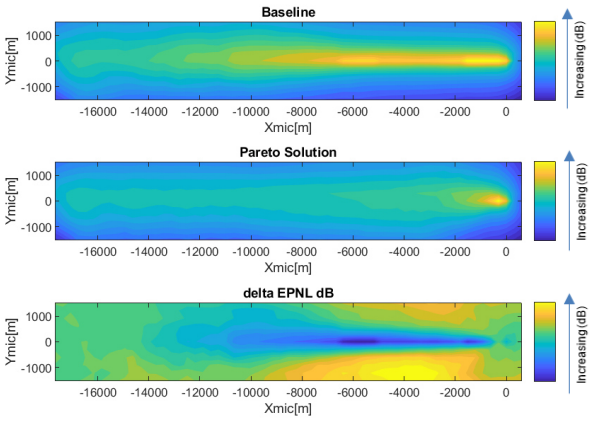

Figure 21 EPNL dB Acoustic Footprint for (a) baseline case (b) optimal pareto solution and (c) the delta EPNL between the two footprints

These results show that the EPNL dB metric strongly optimises for reduced noise at the optimisation microphone positions at the expense of the surrounding noise levels. Further analysis may need to consider an alternative microphone grid array, which may be used to minimise overall ground footprint EPNL values.

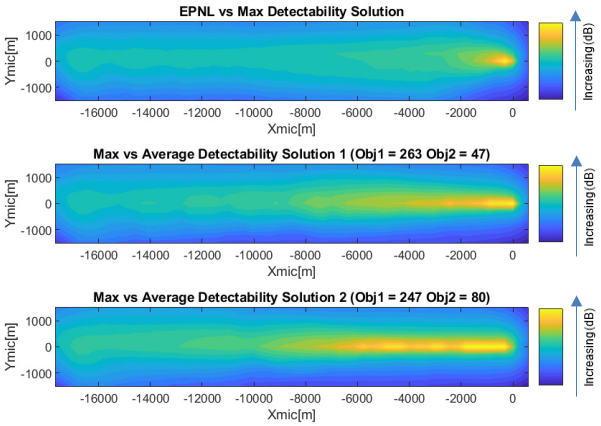

Figure 22 EPNL dB footprints for the optimal pareto solutions for (a) EPNL vs Max Detectability, (b) Max vs Average detectability Obj1 = 263, Obj2 = 47 and (c) Max vs Average Detectability Obj1 = 247, Obj2 = 80

The footprint also shows that in order to reduce the onground noise footprint over the total length of the descent path, the noise to the right of the helicopter (starboard side) must increase, as a result of the change in helicopter trim condition. The EPNL dB footprint also shows, unlike the SEL dB analysis in the previous section, an increased section of noise between x positions -7000m and -5000m. This is likely due to the tonality correction factor applied in the EPNL calculation, and shows that there can be a noticeable difference between the two measurement variables.

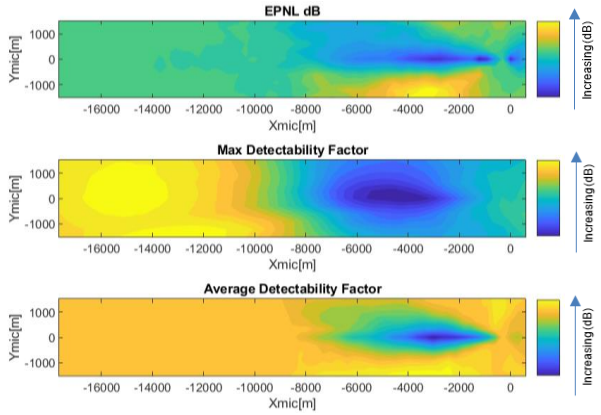

Figure 23 Delta comparison between the EPNL vs Max detectability and the Average vs Max detectability (Obj1 = 247, Obj2 = 80) solutions, where –ve values refer to a reduction in the former for (a) EPNL dB, (b) Max detectability factor, (c) Average detectability factor

A further analysis, considering the EPNL dB footprints of the two optimal pareto solutions for the same microphone array case is given in Figure 22. These results show that the EPNL dB footprint is considerably higher along the total footprint when not optimised – while the SEL footprint analysed above in section 1 shows a correlated reduction with the optimisation of the detectability objectives. This shows that annoyance and detectability objectives do not necessarily positively correlate, and the balance between detectability and annoyance metrics must be further considered.

A further analysis into the difference in optimised detectability factors over the noise footprint of the helicopter when either EPNL dB and detectability, or purely detectability metrics are considered is shown in Figures 23 and 24. The results show a reduction in noise for optimised EPNL dB vs Max detectability threshold towards the end of the flight trajectory, but with a slight increase at higher altitudes. The average detectability threshold shows a decrease in value across the full footprint, with a considerably higher reduction over the microphone array mic positions.

Since the optimal solutions for the Max vs Average detectability factor optimisation, using microphone array 1, maximise the maximum threshold value – this suggests that the EPNLdB metric must give a considerably more averaged parameter. The calculation procedure for EPNL dB correlates with this observation, and suggests that the EPNL dB metric positively correlates with the average detectability threshold.

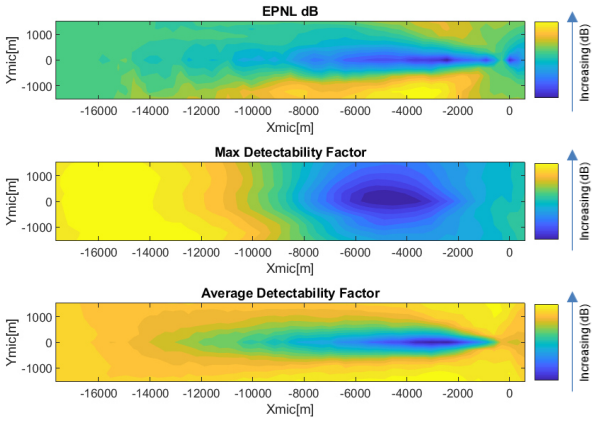

Figure 24 Delta comparison between the EPNL vs Max detectability and the Average vs Max detectability (Obj1 = 263, Obj2 = 47) solutions, where –ve values refer to a reduction in the former for (a) EPNL dB, (b) Max detectability factor, (c) Average detectability factor

These results show that the precise sound quality metrics used to optimise the trajectory for detectability can have a large effect on the overall outcome. The relationship between the optimised values needs to be investigated further, in order to produce an optimisation procedure which is able to maximise the positive correlation between multiple

sound quality metrics and thus may be able to directly improve multiple sound qualities simultaneously.

6 CONCLUSION AND OUTLOOK

This paper has performed a review of recent literature on psychoacoustics and detectability. Based on this knowledge, an existing trajectory optimisation algorithm has been adapted to optimise for detectability. The optimisation tool currently performs a conventional approach trajectory, and is built on classical signal detection theory – assuming zero background noise. It performs an optimisation based on average and maximum threshold values over an array of microphones specified at the beginning of the optimisation procedure. An acoustic database of an LH helicopter was also developed, and fed into the optimisation tool chain.

This paper has analysed three different optimisation array configurations, directly below, to the right, and in front of the helicopter final landing point. The investigations have yielded encouraging results, giving an insight into the complex helicopter noise signature, and the way it can be tuned through its flight path to account for human aural perception.
Results from the optimisation tool have shown that it is possible to optimise the helicopter trim condition in flight to reduce helicopter detection and noise directivity in multiple directions. Results also showed that for initial analyses, SEL and EPNL can be accurate and powerful tools for optimisation procedures to gauge annoyance in the absence of more sophisticated SQ metrics.

While the initial approach to optimising detectability, as given within this paper, was successful and the analysis showed that it was able to both control directivity and calculate detection ranges, the approach has still great potential for extension.

Work could be done to extend the analysis to a full range of psychoacoustic sound metrics, and introduce localisation. An extension to include background noise within the model, and investigate the effects of different masking noise on the perception of the helicopter noise thresholds would be particularly interesting, given the complexity of the helicopter acoustic signature. Experimental analysis of the effectiveness of these metrics would also be needed to provide further confidence in the model results. The approach currently only calculates detectability for the approach condition – this could also be extended to look at both steady and unsteady maneouvres, at a wider range of speeds and trim envelopes.

7 REFERENCES

[1] D. M. Leverton, "Helicopter Noise: What is the Problem?," *VERTIFLIGHT,* March/April 2014.

[2] E. Ungar, "A Guide for Predicting the Aural Detectability of Aircraft," Air Force Flight Dynamics Lab, March 1972.

[3] L. Cruz, A. Massaro, S. Melone and A. D'Andrea, "Rotorcraft Multi-Objective Trajectory Optimization for Low Noise Landing Procedures," *European Rotorcraft Forum,* 2012.

[4] S. L. Padula, C. L. Burley, D. D. Boyd Jr. and M. A. Marcolini, "Design of Quiet Rotorcraft Approach," Langley Research Center, Hampton, Virginia.

[5] E. E. Ungar, "A Guide for Predicting the Aural Detectability of Aircraft," US Air Force Dynamics Laboratory, March 1972.

[6] S. Fidell, "Predicting Aural Detectability of Aircraft in Noise Backgrounds," Air Force Flight Dynamics Laboratory, 1976.

[7] E. M. Hoglund and e. al, "Human Validation of the AUDIB Auditory Perception," Air Force Research Laboratory, 2008.

[8] E. M. Hoglund and e. al, "Human Validation of the AUDIB Auditory Perception Model for Rotarywing Aircraft," U.S. Air Force Research Laboratory, 2008.

[9] S. Krishnamurthy, A. Christian and S. A. Rizzi, "Psychoacoustic Test to Determine Sound Quality Metric Indicators," *INTERNOISE Impact of Noise Control Engineering,* no. 26-29 August , 2018.

[10] J. Molino, "Should Helicopter Noise Be Measured Differently From Other Aircraft Noise? - A Review of the Psychoacoustic Literature," NASA Contractor Report, 1982.

[11] M. A. Boucher, A. W. Christian and S. Krishnamurthy, "A perceptual evaluation of the efficacy of Sound Exposure Level," VFS International 76th Annual Forum, Virginia, 2020.

[12] H. Fastl and E. Zwicker, Psychoacoustics, Facts and Models, Edition 3, Springer, 2007.

[13] N. Yasui and M. Miura, "Relationship between fluctuation strength and detectability of alert sounds for hybrid and electric vehicle," in *Institute of Noise Control Engineering, INTER-NOISE and NOISE-CON Congress and Conference Proceedings,*, Hong Kong, 2017.

[14] L. Steinbach and M. E. Altinsoy, "Prediction of Detectability of Synthesized Vehicle Sounds Using Logistic Regression," October 2018.

[15] T. Van Rentergham et al, "Annoyance, detection and recognition of wind turbine noise," *Science of The Total Environment,* Vols. 456-457, pp. 333-345, July 2013.

[16] J. B. Ollerhead, "Helicopter Aural Detectability," U.S Army Air Mobility Research and Development Laboratory, Fort Eustis, Virginia, 1971.

[17] E. Zwicker and H. Fastl, Psychoacoustics, Facts and Models, Springer Science and Business Media, 1990.